



Influences of fly ash on magnesium oxychloride mortar

C.K. Chau, James Chan, Zongjin Li *

Department of Civil Engineering, The Hong Kong University of Science and Technology, Clear Water Bay, Kowloon, Hong Kong, China

ARTICLE INFO

Article history:

Received 17 April 2007

Received in revised form 7 February 2009

Accepted 11 February 2009

Available online 25 February 2009

Keywords:

Magnesium oxychloride

Cement

Phase diagram

Fly ash

Repair mortar

ABSTRACT

The application of magnesia-based construction materials draws much research interests nowadays due to the ever increasing awareness of environmental protection. By incorporation of fly ash into magnesium oxychloride (MOC) cement, an energy efficient and environmentally friendly repair material can be formed for successful industrial applications. In the current research, an appropriate formulation of the MOC matrix with a suitable combination of the molar ratios MgO/MgCl_2 and $\text{H}_2\text{O}/\text{MgCl}_2$ has been characterized by using phase diagram, X-ray diffractograms and scanning electronic microscope. Subsequently the influences of fly ash on the properties of both MOC cement and mortar are investigated. It is found that the incorporation of fly ash can enhance the workability or fluidity, retard the setting time, and improve the water resistance of the MOC mortars. With the enhanced performance and a slightly expansive nature, the MOC mortars incorporated with fly ash has a good potential to be used as a repairing material.

© 2009 Published by Elsevier Ltd.

1. Introduction

As an air-dried magnesia-based cementing material, magnesium oxychloride (MOC) cement [1] was developed shortly after the invention of Portland cement. With a through solution reaction [2–4] at ambient temperature, the MOC system is a typical ternary system with magnesium oxide, magnesium chloride and water the three major reaction components. The two main chemical composition phases produced in the ternary system are $3\text{Mg}(\text{OH})_2 \cdot \text{MgCl}_2 \cdot 8\text{H}_2\text{O}$ (phase 3) and $5\text{Mg}(\text{OH})_2 \cdot \text{MgCl}_2 \cdot 8\text{H}_2\text{O}$ (phase 5) [5,6]. The well crystallized needle-like phase 5 of chemically bonded MOC has been described as scroll-tubular whiskers [7]. The mechanical interlocking and unique microstructure resulting from the intergrowth of the crystals is a major source for the strength development of MOC cement [8]. Therefore, the physical properties of MOC cement and mortar depend largely on the phases formation and subsequently on the appropriate proportions of the starting materials.

It is well known that MOC cement has many properties superior to the ordinary Portland cement. By virtue of its elastic and acoustic properties, and attractive marble-like appearance, MOC cement is used for rendering wall insulation panels, interior plasters and exterior stuccos, and decorative panels [9]. Some other commercial and industrial applications of MOC cement are industrial flooring [10], fire protection [11], grinding wheels and light weight concrete [12]. The excellent performance of MOC cement including rapid setting and hardening, good resistance to abrasion and

chemicals, as well as remarkable bonding ability to large amounts of different inert fillers [13] makes it an attractive candidate of binding materials for repair mortar.

Moreover, MOC cement draws much research interests recently due to the energy saving consideration [14] as it can be used as a Portland cement replacement on many occasions. The production of light burnt MgO used in MOC requires a much lower calcination temperature compared to that for Portland cement, thus reducing vast amount of energy consumption and favorable for the sustainable development of the building industry. Besides, generated during the combustion of coal for energy production, fly ash is one of the major industrial by-products and being utilized in the construction industry for decades. By incorporation of fly ash into MOC cement, an energy saving and environmentally friendly repair material can be formed for industrial applications. In addition, water resistance of MOC system is a key issue in the research before MOC related products could be utilized in the industry [15]. To that end, the effects of the fly ash on both MOC cement and mortar, including phase composition, flow property, setting time, strength development, water resistance as well as volume stability, have been investigated.

In this paper, the phase compositions and microstructures of MOC pastes were evaluated by phase diagram, X-ray diffractograms and scanning electronic microscope. As a result, a cement matrix with a suitable combination of the molar ratios MgO/MgCl_2 and $\text{H}_2\text{O}/\text{MgCl}_2$ was chosen for producing MOC mortars to ensure the formation of needle-shaped phase 5 crystals in the ternary MOC system. The experimental studies show that the incorporation of fly ash can enhance the workability or fluidity, retard the setting time, secure the volume stability, and improve the water resistance of the MOC mortars.

* Corresponding author. Tel.: +86 852 2358 8751.

E-mail address: zongjin@ust.hk (Z. Li).

2. Experimental programme

The magnesium oxide used in this study was calcined magnesite powder with a purity of 96% from Jinan, Shandong Province, China. The magnesium chloride employed was hygroscopic hexahydrate crystal, $\text{MgCl}_2 \cdot 6\text{H}_2\text{O}$, with a purity of 98% from Israel. As well, Class F (ASTM C618) fly ash from CLP (China Light & Power Company Ltd., HK) was used. The chemical compositions of the raw materials analyzed by X-ray fluorescence spectrometer (JEOL JSX-3201Z) are listed in Table 1. As a fine aggregate, natural river sand with a fineness modulus of 2.3 was employed for preparing MOC mortars. For the ternary system of MgO – MgCl_2 – H_2O at ambient temperature, two molar ratios of MgO/MgCl_2 and $\text{H}_2\text{O}/\text{MgCl}_2$ are used for preparation of the materials. To find out an appropriate formulation of the binding matrix for the mortars, MOC cement pastes with different combinations of the two molar ratios were prepared as shown in Table 2. Finally, the mixture design of the MOC mortars blended with different contents of fly ash is shown in Table 3.

For each mixture assigned in the above tables, cubic specimens with a size of $40 \times 40 \times 40$ mm were prepared for strength measurement and water resistant test, and prisms with a size of $25 \times 25 \times 280$ mm for drying shrinkage monitoring. The specimens were cast in steel moulds with vibration compaction followed by air curing at a temperature of 24 ± 1 °C and under a relative humidity of $60 \pm 5\%$. The crystalline phases of the MOC pastes were identified by powder X-ray diffraction (XRD, Philips PW 1830) patterns using Cu $K\alpha$ radiation. The powder samples were prepared by crushing the cubic specimens and passing the powder through a sieve with a screen aperture of 75 μm . The morphology and microstructure of the MOC pastes were characterized by scanning electron microscopy (SEM, JSM-6300) on fractured surface with gold coating.

The fluidity of the MOC mortars incorporated with fly ash was evaluated by flow table method (GB 2419). It measures the diameter of a conical frustum, of the mortars with an original base diameter of 100 mm, after the flow table moving up and down 30 times through a height of 25 mm in 30 s. The setting time was determined with the Vicat apparatus, while the volume stability was gauged by the length change of the prism specimens under 28 °C and 50% RH. In addition, the water resistance of the MOC mortars was indexed by the strength retention coefficient, R , which can be estimated by

$$R = S_x/S_y \quad (1)$$

where S_x is the residual strength of the specimen after soaking in water for a period of time, and S_y the strength of the reference specimen cured in air.

The test regime for water resistant of the MOC mortars adopted in this study was scheduled as follows. After air curing of 14 days (A14), part of the specimens was soaked in distilled water for 28 days (A14W28) while part of the specimens was kept curing in air until 42 days (A42). Then residual strength of the specimens after water soaking (A14W28) was measured and compared to the reference strength of the specimens cured in air (A14 and A42) for the calculation of the strength retention coefficient.

Table 1
Chemical compositions of the raw materials used.

Materials	Mass fraction (%)											
	MgO	Al_2O_3	SiO_2	P_2O_5	SO_3	K_2O	CaO	MnO	Fe_2O_3	MgCl_2	H_2O	CaCl ₂
MgO	96.6	0.11	0.76	0.04	0.16	0.02	1.41	0.14	0.76	–	–	–
Fly ash	2.93	20.1	49.9	0.94	1.13	1.98	8.53	0.23	11.8	–	–	–
$\text{MgCl}_2 \cdot 6\text{H}_2\text{O}$	–	–	–	–	–	–	–	–	–	45.8	52.0	1.3

Table 2

Mixture design of the MOC cement pastes.

Mixtures	Molar ratios		Fly ash ^a
	$[\text{MgO}/\text{MgCl}_2]$	$[\text{H}_2\text{O}/\text{MgCl}_2]$	
#1	3.6	12	–
#2	4.7	12	–
#3		14	–
#4		16	–
#5	7.8	20	–
#6			30%

^a By weight of MgO.

Table 3

Mixture design of the MOC mortars.

Mixtures	Powders		Water to powder ratio	Sand to powder ratio
	$[\text{MgO}/\text{MgCl}_2]^a$	Fly ash ^b (%)		
#7	4.7	–	0.47	1.50
#8		10		
#9		20		
#10		30		

^a Molar ratio.

^b By weight of MgO.

3. Results and discussion

3.1. Selection of MOC matrix

The phase diagram of the ternary MOC system at ambient temperature is demonstrated in Fig. 1 with the composition points of the paste mixtures (Table 2) indicated. With different combinations of the two molar ratios, MgO/MgCl_2 and $\text{H}_2\text{O}/\text{MgCl}_2$, the composition points of the three MOC pastes (mixtures #1, #3 and #5) are located in three adjacent compatibility triangles (points 1, 2 and 3 in Fig. 1b) with different phase assemblages. According to the level rule of the phase diagram [16], the phase assemblage of the mixture #1 would be both phase 3 and phase 5 coexistent, the mixture #3 mostly phase 5, and the mixture #5 both phase 5 and brucite present. The corresponding X-ray diffractograms of the three MOC pastes are stacked in Fig. 2 showing good agreement with the above observations. With a fixed molar ratio of MgO/MgCl_2 , the composition points of the mixtures with different molar ratios of $\text{H}_2\text{O}/\text{MgCl}_2$ will be moving along a straight line, extending towards the H_2O apex of the phase diagram. That is the case for the mixtures #2, #3 and #4 with the same molar ratio of MgO/MgCl_2 of 4.7 and different molar ratios of $\text{H}_2\text{O}/\text{MgCl}_2$ of 12, 14 and 16, correspondingly.

On one hand, with the least water content among the mixtures #2, #3 and #4, the composition point of the mixture #2 falls into the compatibility triangle of MgO –phase 3–phase 5. The mixture #2 should, therefore, have both phase 3 and phase 5 coexistent similar to that of the mixture #1 as shown in Fig. 2. On the other hand, with a higher water content as compared to the other two mixtures, the mixture #4 should have mainly phase 5 as well as

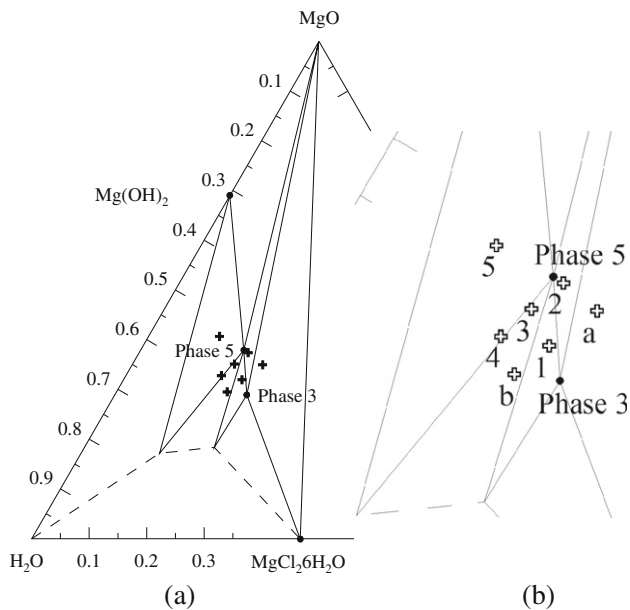


Fig. 1. Phase diagram of the ternary MOC system: (a) isothermal section at 25 ± 3 °C (the dashed line indicates the approximate limits of homogeneous gel formation); and (b) magnified portion of (a) with labeled composition points of the MOC pastes (points 1–5 for the mixtures #1–#5).

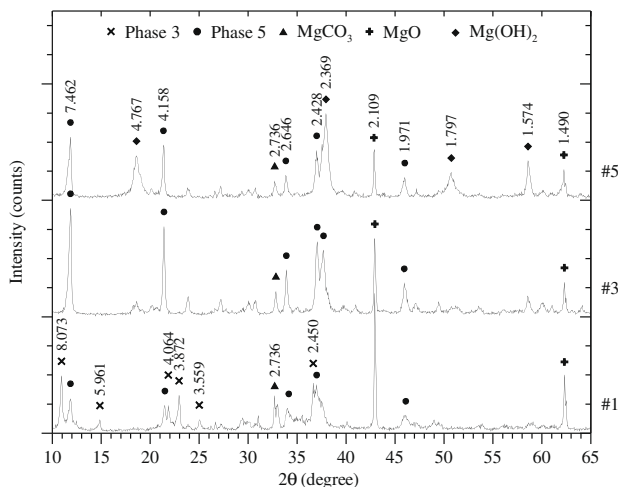


Fig. 2. Typical X-ray diffractograms of the MOC cement pastes.

more amorphous gel phase (points 2, 3 and 4 in Fig. 1b). Moreover, with an addition of fly ash of 30% by weight of MgO while keeping the other constituents fixed, the relative phase composition of the mixture #6 is different to that of the mixture #5 as compared in Fig. 3. Although they both have the same phase assemblage of phase 5, brucite and MgO residual, the relative amounts are different. Obviously, the total amount of brucite in the mixture #6 is less and MgO residual is more as compared to that in the mixture #5. As a result, it is believed that the growth of brucite in the MOC pastes can be inhibited to a certain extent by the incorporation of the mineral admixture of fly ash. The beneficial effect of this phenomenon will be shown more clearly in the following section regarding the water resistance of MOC mortar.

Furthermore, with a higher molar ratio of MgO/MgCl₂, more brucite would be produced, while with a lower molar ratio of MgO/MgCl₂, the amount of the phase 3 would be increased or even a MOC paste with dominant phase 3 would be established (point a

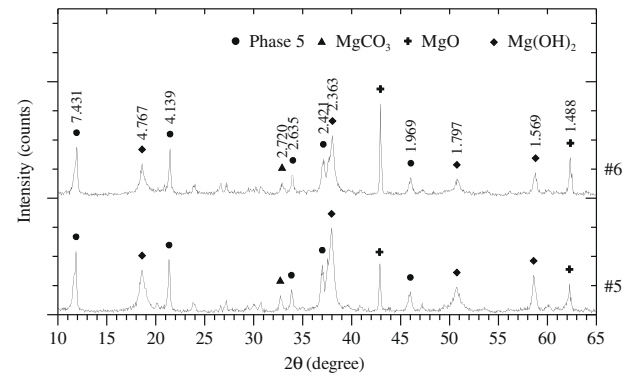


Fig. 3. Effect of fly ash on phase composition of the MOC pastes.

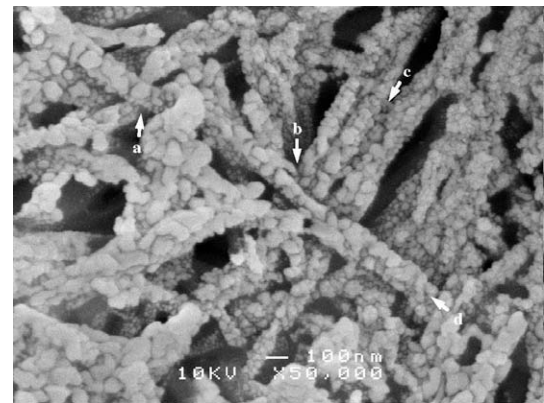


Fig. 4. Interlaced microstructure of needle-shaped crystals of the mixture #3.

in Fig. 1b). With a low molar ratio of MgO/MgCl₂ and a high molar ratio of H₂O/MgCl₂, the gel phase will be increased as indicated by point b in Fig. 1b. The phase 5, however, is more preferred as it is attributed to the strength development of MOC cement. The morphology of the needle-shaped phase 5 crystals of the mixture #3 under SEM is revealed in Fig. 4. The intergrowth and interlaced microstructure (arrows a and b) of the bundled needle-shaped (arrows c and d) crystals are attributed to the mechanical interlocking leading to enhanced strength development. Therefore, the formulation of the MOC paste #3 was chosen as the binding matrix for the mixture design of MOC mortars incorporated with fly ash.

3.2. Effects of fly ash on MOC mortars

Based on the formulation of the MOC paste #3 and a sand to powder weight ratio of 1.5, four MOC mortars with different contents of fly ash (Table 3) were prepared and evaluated. The favorable effect of fly ash on the fluidity and setting time of the MOC mortars are shown in Fig. 5. It can be seen that the workability of the MOC mortars is enhanced as the content of fly ash increased due to the lubricating effect of the spherical shaped fly ash particles. As well, both the initial and final setting times of the MOC mortars are retarded by the addition of fly ash and following a similar trend of the fluidity enhancement. The improved workability and prolonged setting time would be beneficial for the MOC mortars as a repair material.

The influence of the incorporation of fly ash on strength development of the MOC mortars is shown in Fig. 6. It can be seen that the compressive strength of the MOC mortars decreased with the increase of amount of fly ash addition. The strength development of the control mixture #7 is rapid and reaches its stable stage after

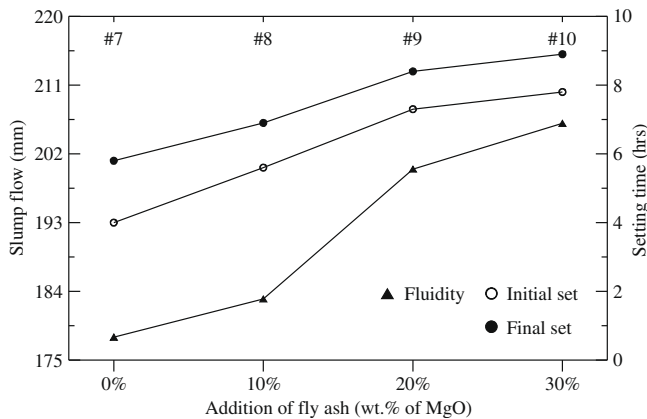


Fig. 5. Fluidity and setting time of the MOC mortars blended with fly ash.

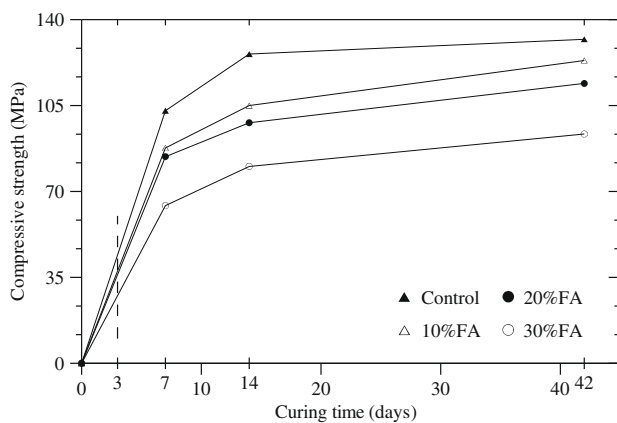


Fig. 6. Effect of fly ash on strength development of the MOC mortars.

only 2 weeks of air curing. However, the other mixtures with incorporation of fly ash (#8–#10) seems still continue to grow in strength after 6 weeks of air curing. It should be pointed out that, from a practical point of view, at a strength level of over 20 MPa after 3 days curing (the dashed line in Fig. 6), the MOC mortars incorporated with fly ash are strong enough to carry pedestrian and any type of rubber-wheeled traffic in the case of concrete carriageway repair.

The result of the water soaking tests as plotted in Fig. 7 exhibits that the water resistance of the MOC mortars would be dramati-

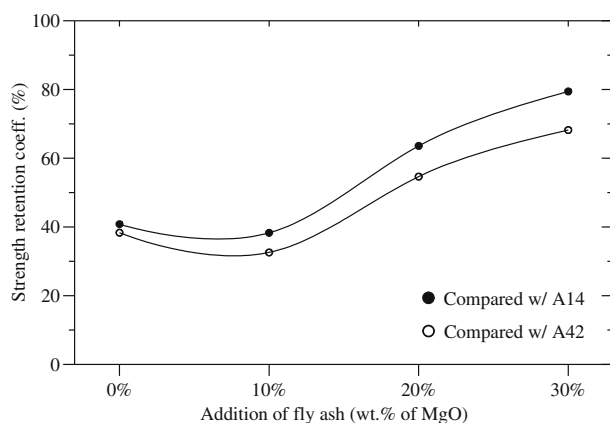


Fig. 7. Water resistance of the MOC mortars with fly ash.

cally boosted when appropriate amount of fly ash is utilized. For the MOC mortar incorporated with fly ash of 30% by weight of MgO, the strength retention coefficient is raised from merely 40% up to about 80% when compared to the reference strength at 14-day air curing (A14). The improvement of the water resistance of the MOC mortars with fly ash incorporation may be due to the amorphous aluminosilicate gel formed by the pozzolanic reaction of the reactive SiO_2 and Al_2O_3 contents of fly ash under the alkaline condition of MOC system. With a large surface area, the well dispersed fly ash particles would form a network of the aluminosilicate gel weaved with the microstructure of the MOC crystals. As a result, the water shy MOC phases would be protected to a certain extent by the surrounding spherical fly ash particles and water insoluble aluminosilicate gel.

The X-ray diffractograms of the specimens of the mixtures #7 and #10 after water soaking are compared in Fig. 8. It shows that the residual phase compositions of the two mortars with and without fly ash are quite different. For the control mixture #7 of plain MOC mortar, the main MOC phases are disappeared and only brucite left. While for the mixture #10 with 30% FA by weight of MgO, significant amount of phase 5 is still remained with inevitably brucite also found. That can be used to explain why the mixture #10 has a much higher strength retention coefficient. It is understood that the MOC phases (phase 3 and phase 5) are not stable in water and would be decomposed into brucite after a sustained period of

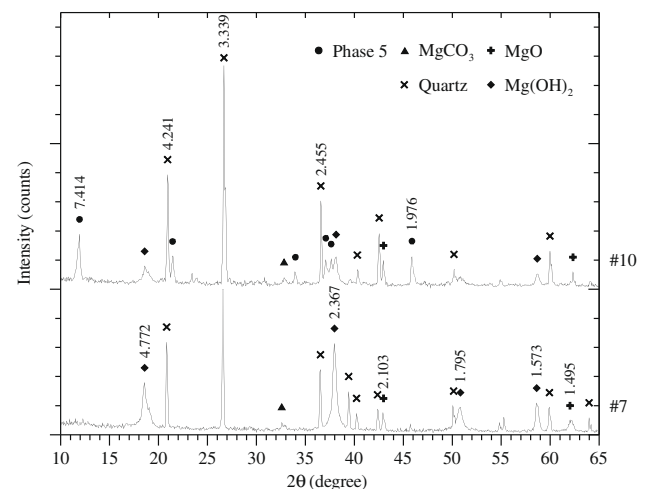


Fig. 8. X-ray diffractograms of the MOC mortars after water soaking.

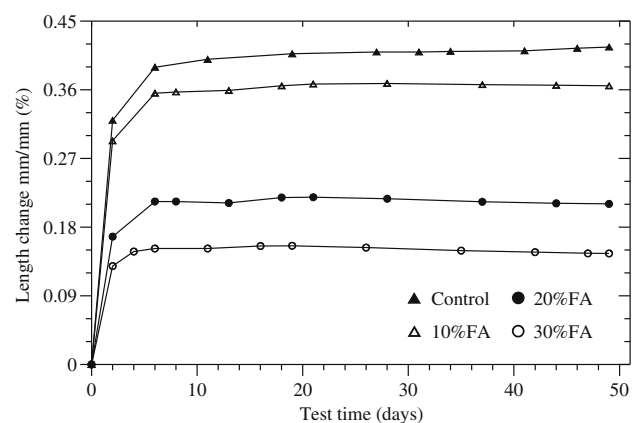


Fig. 9. Drying shrinkage of the MOC mortars with different contents of fly ash.

exposure to water. If the formation of brucite was limited, then the rate of the decomposition would be at least postponed, if not totally prevented. Consequently, the inhibitability of brucite growth by fly ash (Fig. 3) as shown in the previous section could also be attributed to the enhancement of water resistance of the MOC mortars.

Finally, the influence of fly ash incorporation on volume stability of the MOC mortars are plotted in Fig. 9 which shows the length change of the prism specimens under drying conditions. It demonstrates that the MOC mortars are in general expansive and most of the expansion taking place in the first week after casting. Besides, it is believed that the expansion of the mortars may only come from the MOC matrix. The fly ash incorporation reduces amount of expansion and the more amount incorporated, the more the deduction as shown in Fig. 9. A slightly expansive nature of the MOC mortars is favorable for being a repair mortar to avoid crack and premature failure due to drying shrinkage.

4. Conclusions

The influences of fly ash on the properties of both MOC cement and mortars are investigated in this study. By incorporating fly ash up to 30% by weight of MgO in the MOC mortars, the workability or fluidity is enhanced, the setting time retarded, and more importantly the water resistance improved, although the final compressive strength decreased. The improvement of the water resistance of the MOC mortars incorporated with fly ash may be attributed to the amorphous alumino-silicate gel formed by the pozzolanic reaction of the reactive SiO_2 and Al_2O_3 contents of fly ash under the alkaline condition of MOC system. Moreover, the experimental results show that the growth of brucite in the MOC matrix can be inhibited by fly ash. Consequently, the rate of the decomposition of the MOC phases under water would be at least postponed, if not totally prevented. Finally, a slightly adjustable expansive nature of the MOC mortars incorporated with different amount of fly ash is favorable for being a repair mortar to compensate the effect of drying shrinkage.

Acknowledgements

The partial financial support from China Ministry of Science & Technology under Grant of 2009CB623200 is greatly acknowledged. Special thanks is extended to Mrs. Christine Cheung for her conscientious assistance in XRD measurements.

References

- [1] Sorel S. On a new magnesium cement. *C R Hebd Acad Sci* 1867;65:102–4.
- [2] Bilinski H, Matkovic B, Mazuravic C, Zunic TA. The formation of magnesium oxychloride phases in the system of $\text{MgO-MgCl}_2\text{-H}_2\text{O}$ and $\text{NaOH-MgCl}_2\text{-H}_2\text{O}$. *J Am Ceram Soc* 1984;67(4):266–9.
- [3] Menetrier-Sorrentino D, Barret P, Saquat S. Investigation in the system $\text{MgO-MgCl}_2\text{-H}_2\text{O}$ and hydration of Sorel cement. In: *Proceedings of the 8th ICCS*, vol. 4, Rio de Janeiro; 1986. p. 339–43.
- [4] Deng D, Zhang C. The formation mechanism of the hydrate phases in magnesium oxychloride cement. *Cem Concr Res* 1999;29(9):1365–71.
- [5] Demediuk T, Cole WF, Heuber HV. Studies of magnesium and calcium oxychlorides. *Aust J Chem* 1955;8(2):215–33.
- [6] Cole WF, Demediuk T. X-ray, thermal and dehydration studies on magnesium oxychloride. *Aust J Chem* 1955;8(2):234–51.
- [7] Tooper B, Cartz L. Structure and formation of magnesium oxychloride Sorel cements. *Nat Phys Sci* 1966;211:64–6.
- [8] Matkovic B, Young JF. Microstructure of magnesium oxychloride cements. *Nat Phys Sci* 1973;246:79–80.
- [9] de Henau P, Dupas M. Study of the alternation in acropolis monuments. In: *Proceedings of second international symposium on the deterioration of building stone*, Athens; 1976. p. 319–25.
- [10] Li G, Yu Y, Li J. Experimental study on urban refuse/magnesium oxychloride cement compound floor tile. *Cem Concr Res* 2003;33(10):1663–8.
- [11] Montle JF, Mayhan KG. Magnesium oxychloride as a fire retardant material. *J Fire Flammabil/Fire Retard Chem* 1974;1:243–54.
- [12] Biel TD, Lee H. Magnesium oxychloride cement concrete with recycled tire rubber. *Transportation Research Record No. 1561*, Washington (DC); 1996. p. 6–12.
- [13] Siddique R, Naik TR. Properties of concrete containing scrap tire rubber – an overview. *Waste Manage* 2004;24(6):563–9.
- [14] Li Z, Ding Z, Zhang Y. Development of sustainable cementitious materials. In: *Proceedings of the international workshop on sustainable development and concrete technology*; 2004. p. 55–76.
- [15] Chan James, Li Zongjin. Influence of fly ash on the properties of magnesium oxychloride cement. In: *Proceedings of the international symposium of measuring, monitoring and modeling concrete properties*; 2006. p. 347–52.
- [16] McHale AE. Phase diagrams and ceramic processes. New York: Chapman & Hall; 1998. 184p.